GPS Solut (2016) 20:641–654
DOI 10.1007/s10291-015-0474-0

ORIGINAL ARTICLE

Long-term soil moisture dynamics derived from GNSS interferometric reflectometry: a case study for Sutherland, South Africa

Sibylle Vey[1] · Andreas Güntner[1] · Jens Wickert[1] · Theresa Blume[1] · Markus Ramatschi[1]

Received: 10 December 2014 / Accepted: 4 July 2015 / Published online: 23 July 2015

Abstract Soil moisture is a geophysical key observable for predicting floods and droughts, modeling weather and climate and optimizing agricultural management. Currently available in situ observations are limited to small sampling volumes and restricted number of sites, whereas measurements from satellites lack spatial resolution. Global navigation satellite system (GNSS) receivers can be used to estimate soil moisture time series at an intermediate scale of about 1000 m^2. In this study, GNSS signal-to-noise ratio (SNR) data at the station Sutherland, South Africa, are used to estimate soil moisture variations during 2008–2014. The results capture the wetting and drying cycles in response to rainfall. The GNSS Volumetric Water Content (VWC) is highly correlated ($r^2 = 0.8$) with in situ observations by time-domain reflectometry sensors and is accurate to 0.05 m^3/m^3. The soil moisture estimates derived from the SNR of the L1 and L2P signals compared to the L2C show small differences with a RMSE of 0.03 m^3/m^3. A reduction in the SNR sampling rate from 1 to 30 s has very little impact on the accuracy of the soil moisture estimates (RMSE of the VWC difference 1–30 s is 0.01 m^3/m^3). The results show that the existing data of the global tracking network with continuous observations of the L1 and L2P signals with a 30-s sampling rate over the last two decades can provide valuable complementary soil moisture observations worldwide.

Keywords GNSS · Reflectometry · Soil moisture · Signal-to-noise ratio

✉ Sibylle Vey
vey@gfz-potsdam.de

[1] GFZ German Research Centre for Geosciences, Telegrafenberg, 14473 Potsdam, Germany

Introduction

Soil moisture is a fundamental component in the hydrological cycle. The moisture in the uppermost soil layer directly influences evaporation and thus the water and heat fluxes between the soil and the atmosphere. Soil moisture can have a relevant feedback with air temperature and precipitation dynamics (Seneviratne et al. 2010). Hence, observations of soil moisture are very valuable for weather forecast and climate studies (Drusch 2007) and are also important for irrigation management and flood prediction (Brocca et al. 2010; Wanders et al. 2014). Furthermore, soil moisture plays an important role in contaminant and nutrient transport and influences the emission of greenhouse gases (Schaufler et al. 2010).

However, obtaining soil moisture data at the field scale is a challenge since continuous observations are generally point measurements with small sampling volumes and the strong heterogeneity of the subsurface introduces large uncertainties in averaging techniques (Perry and Niemann 2008). Observations from remote sensing satellites, e.g., the soil moisture and ocean salinity (SMOS) mission or the planned soil moisture active passive (SMAP) mission, on the other hand, have the disadvantage of large footprints with a resolution of 10 or 50 km for SMAP and SMOS, respectively (Wang and Qu 2009; Entekhabi et al. 2008; Dorigo et al. 2014).

The use of data from the global navigation satellite systems (GNSS) for remote sensing based on utilizing earth reflected signals was proposed in a pioneering work by Martin-Neira (1993). The dual-frequency GNSS signals are in the L-Band with wavelengths of, e.g., 19.05 and 24.45 cm for the GPS system. Several studies have shown that, with specially designed GNSS antenna and receiver systems, it is possible to estimate near-surface soil moisture

(Zavorotny et al. 2003; Masters et al. 2002; Katzberg et al. 2005; Egido et al. 2014). These measurements used custom designed systems based on two GNSS antennas: one tracking the direct signals from the satellites and the other oriented toward the ground to track the reflected signal. The reflected signal is also referred to as multipath.

Rodriguez-Alvarez et al. (2009) and Alonso-Arroyo et al. (2014) used custom designed single antennas to derive soil moisture signals applying the interference pattern technique (IPT). The IPT is based on the coherent addition of the reflected and the direct signal in a single GNSS antenna. Larson et al. (2008) showed that it is possible to estimate soil moisture with measurements from a standard single ground-based dual-frequency geodetic GNSS receiver, which was set up for geodynamic applications. They demonstrated that these geodetic-type GNSS instruments, which are optimized to track the direct signals from the satellites, could successfully be used to measure the reflected signals too.

The soil moisture retrieval algorithm proposed by Larson et al. (2008) is based on the analysis of power variations of the GNSS signals. The direct signal from the GNSS satellite and the signal reflected by the land surface are simultaneously received at the antenna, and their power is added with consideration of their phase difference. Due to the motion of the GNSS satellites, the simultaneous reception of the direct and coherently reflected signals causes an interference pattern in the signal power. This interference pattern depends on the height difference between the GNSS antenna and the reflection point (Nievinski and Larson 2014). If the soil is wet, the GNSS signal is reflected from a layer just below the land surface while for dry soil, the signal penetrates deeper into the soil and is reflected within a surface layer of up to 7 cm depth (Larson et al. 2010).

The power of the GNSS signal is a standard observable and recorded as signal-to-noise ratio (SNR) additionally to the phase and code observations in standard receiver independent exchange format (RINEX) observation files (Gurtner and Estey 2007). This SNR is the ratio of the GNSS signal power to the measurement noise given in a logarithmic decibel (dB) or decibel-Hertz (dB-Hz) scale. In operational applications, the SNR is used to check the signal quality and characteristics of electromagnetic noise in the close environment of the GNSS station. The SNR mainly depends on the power of the signal transmitted by the GNSS satellite, the antenna gain pattern and the tracking algorithm in the receiver (Larson et al. 2010). Additionally, for low elevation angles, the SNR is also dependent on the power of the reflected signal (Fig. 3). More recent GNSS satellites, i.e., the Block IIR-M and IIF GPS satellites, transmit the new civilian signal L2C (Fontana et al. 2001). For the utilized antenna and receiver, this modernized L2C signal has a 20 dB-Hz higher SNR compared to L2P. Additionally, it is more precise than the L1 signal. Larson et al. (2010) exclusively analyzed SNR data from the L2C signal for soil moisture estimation. However, the L2C signal has been available only since September 2005 when the first Block IIR-M GPS satellite was launched, and only for receivers capable of tracking this signal. Currently, there are seven satellites (PRN 5, 7, 12, 15, 17, 29, 31) transmitting the L2C signal but 24 satellites transmitting L2P only. Thus, the number of observations in a given time and the length of the time series increases significantly if the L2P signal can be used as well.

We present soil moisture estimates based on GNSS interferometric reflectometry for the longest time series published to date. We validate soil moisture estimates derived from L1, L2P and L2C SNR data with in situ time-domain reflectometry (TDR) measurements. Furthermore, we investigate whether data from older GNSS satellites, i.e., the Block IIA and IIR GPS satellites, which are transmitting the L1 and L2P signal only, can give reasonable soil moisture estimates for these earlier time periods. Another important issue is the influence of the sampling rate on the soil moisture estimates. Previous studies using SNR for soil moisture estimation are mainly based on GNSS data with a 1 Hz sampling rate (Larson et al. 2008, 2010). However, for a large part of GNSS stations, the archived data are only stored with much lower sampling rate, e.g., 10 or 30 s, to reduce the data volume. For stations of the International GNSS Service (IGS), the high-rate 1 Hz GNSS data are only archived for a period of 1 year. We investigate whether historical GNSS observations with a 30-s sampling rate, which extend for several stations back into the early 1990s, could provide a valuable data source for long-term soil moisture estimation.

Site description

The study site is situated at the South African Astronomic Observatory (SAAO) where a gravimetric observatory and a hydro-meteorological monitoring network was set up by GFZ. We have chosen the GNSS station Sutherland (SUTM) in South Africa for our case study because independent soil moisture measurements taken from TDR sensors are available close to the GNSS station for validation (at $\sim$30 m distance). Both datasets, GNSS and TDR, cover the time from December 2008 to September 2014. This provides the unique possibility to validate a GNSS-derived soil moisture time series of nearly 6 years. The station SUTM is located in the Northern Cape Province of South Africa in the Karoo drylands at 32.38°S, 20.81°E and at elevation of 1797 m. The mean annual

rainfall is about 350 mm. Due to its high altitude, temperatures may fall below the freezing point in winter. The subsurface consists of dolerite, covered by a soil layer of 10–40 cm depth. The vegetation is dominated by low shrubs of 20–40 cm height, which cover the ground on average to about 25 %. The bare soil surface in between shrubs is composed of a mixture of fine material and stones. In the surroundings of about 10 m of the GNSS antenna, no shrubs exist and the ground is partly covered by herbs no taller than 3 cm. The station environment is very appropriate to receive reflected GNSS signal from the ground because it is clear of obstruction from mountains, buildings and trees and has a high percentage of bare soil. Additionally, the ground is flat, except for the terrain to the east and south of the GNSS antenna location, where boulders up to a height of about 1.5 m cover the underground gravimetric observatory building (Fig. 1).

GNSS data

The GNSS station SUTM is part of the global tracking network of the IGS. It was originally installed to observe plate tectonics and is currently equipped with a geodetic Javad antenna of the type JAV RINGANT G3T (Javad External GPS L1/L2/L5 choke ring antenna) and a receiver of the type JAVAD TRE G3TH DELTA (Javad 216 channels GPS L1/L2/L2C/L5). Before its upgrade on May 7, 2013, the station was equipped with an AOAD/M T antenna (Allen Osborne Associates, Dorne/Margolin element with choke rings, TurboRogue) and a AOA BENCHMARK ACT receiver (Allen Osborne Associates Benchmark with ACT technology, 12 channels). The SNR is recorded with a precision of 0.1 and 0.25 dB for the AOA BENCHMARK ACT receiver and JAVAD TRE G3TH DELTA receiver, respectively.

The footprint size of reflected GNSS signals on a flat and horizontal ground can be described by the first Fresnel zone as an ellipse with a semimajor axis a and semiminor axis b:

$$a = \frac{b}{\sin e}; \quad b = \sqrt{\frac{\lambda h}{\sin e} + \left(\frac{\lambda}{2 \sin e}\right)^2} \tag{1}$$

where λ represents the GNSS wavelength, h is the height of the antenna phase center above the reflecting surface, and e is the satellite elevation angle (Larson and Nievinski 2012). Figure 2 shows the first Fresnel zone for the satellite tracks of SUTM used in the analysis. For a satellite at an elevation angle of 30°, the ellipse of the Fresnel zone has the dimension of $a = 20$ m and $b = 2$ m. The satellite tracks were selected according to the quality of the reflected signal, which is described in more detail in "Data analysis" section. The major axis of the ellipse is aligned in the direction of the satellite–antenna vector. When the satellite is approaching the horizon on a descending orbit, the ellipse becomes larger and moves away from the antenna. For the GNSS station SUTM with its antenna installed on a pillar of 2 m height, the reflections start at a distance of 70 m from the GNSS antenna and approach until 2 m for a satellite pass from 5° to 30° elevation. The satellite needs about 1 h for this passage.

Fig. 1 Antenna of the GNSS station SUTM, Sutherland, South Africa. A cluster of 42 TDR sensors was installed 20–40 m northeast of the GNSS pillar (*white boxes in the background* are the logger and multiplexer boxes of the TDR system, *black arrows* mark the border of the cluster). In the east and south the top surface consists of boulders from construction material, visible on the *right side* of the photo (photo provided by Chantal Fourier)

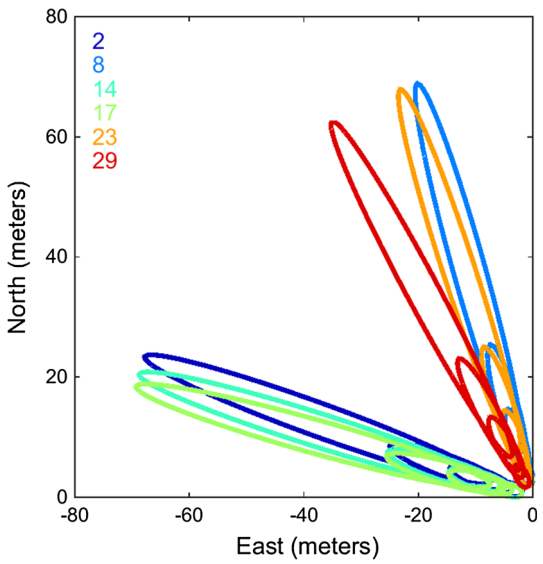

Fig. 2 Areas indicating the coverage of ground tracks of the reflected signals. The Fresnel zones are shown for satellite elevation angles of 5°, 10°, 15° and 30°. The higher the satellite rises, the smaller the ellipsis is and the closer it moves toward the antenna. The *numbers at the top left* are the PRN numbers of the GPS satellites used in this analysis

TDR and climate data, dye tracer experiments

In situ soil moisture monitoring at SUTM is carried out with a cluster of 42 TDR sensors (Campbell Scientific TDR system CS610 with 15 cm rod length and CS645 with 7.5 cm rod length) placed at different soil depths. The TDR cluster is situated 20–40 m northeast of the GNSS station and covers an area of 20 by 20 m (Fig. 1). For this study, we selected 17 TDR near-surface sensors. Nine of these sensors with a rod length of 15 cm were installed vertically from the soil surface, thus providing an average soil moisture value for the top 15 cm of the soil. The other eight TDR sensors are installed horizontally in soil profiles at depths of 10 and 20 cm (four sensors in each depth). The remaining 25 sensors were not considered as they are installed at depths below 20 cm and thus not representative for the near-surface soil moisture sensed by GNSS. Calculation of volumetric water content from the apparent dielectric constant of the soil as measured by the TDR probes is based on the default equation from Topp et al. (1980). A site-specific calibration of the TDR sensors has not been performed. The sensors provide data with 15 min temporal resolution, averaged to daily means for this study similarly to the GNSS-derived soil moisture data. A climate station at the location of the TDR cluster provides time series of air temperature, relative humidity, radiation, wind speed and precipitation. Precipitation is measured by a Hellmann-type rain gauge with a tipping bucket.

Additionally, dye tracer experiments were performed on experimental soil plots at a distance of about 30–40 m from the GNSS station. Using a standard hand-held (herbicide) sprayer, a plot of about 1.2×1.2 m was uniformly sprayed with 25 l of died water with a concentration of Brilliant Blue of 4 g/l. The application period was 2 h, leading to precipitation input of about 17 mm (l/m^2) at an average intensity of 8.7 mm/h. The water completely infiltrated into the soil without generation of surface runoff. On the next day, several vertical soil profiles were excavated and photographed, with blue dye patterns visualizing the water flow paths in the soil.

Data analysis

We analyzed data of the GNSS station SUTM for the period from January 1, 2008, to September 1, 2014. The data of each satellite were analyzed separately. As shown exemplarily for the pass of satellite number two on January 2, 2013, the SNR increases when the satellite is rising and decreases for the descending satellite (Fig. 3 top panel). The SNR variations mainly represent the signal strength of the direct signal. Its signature strongly depends on the antenna gain pattern. The strongest signal can be received when the satellite is in the zenith direction. The reflected signal is only received for satellites with low elevation angles mainly between 5° and 30°. The power of the reflected signal is much smaller than the direct signal. The superposition of reflected and direct signal shows up as interference pattern.

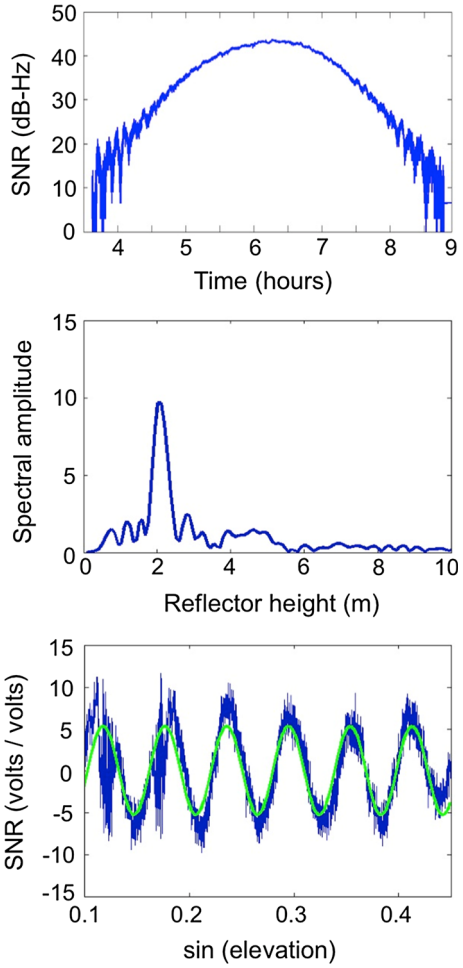

Fig. 3 Signal-to-noise ratio (SNR) of the SUTM measurements for the GPS satellite PRN 2 on January 1, 2013, *top panel* shows the SNR of the complete signal (direct and reflected), *middle panel* represents the SNR of the reflected signal converted to volts/volts for reasons of linearity, *bottom panel* shows the Lomb–Scargle periodogram of the SNR from the reflected signal as shown in the *middle panel*

Our signal analysis generally follows the procedure proposed by Larson et al. (2010). We fit a second-order polynomial to the SNR. By subtracting this polynomial from the SNR data, we isolate the interference pattern. This pattern represents the reflected signal and is therefore referred to as multipath component. We analyze the SNR of the multipath component for satellites with elevation angles ranging between 5° and 30°. For the reason of linearity, we convert the amplitude of the SNR, which is

given in logarithmic dB-Hz units, into volts using the conversion: $\mathrm{SNR}\left(\frac{\mathrm{volts}}{\mathrm{volts}}\right) = 10^{\frac{\mathrm{SNR(dBHz)}}{20}}$. The SNR of the multipath component shows a periodic signature, which is a function of the satellite elevation angle e (Fig. 3 middle panel). When $\sin e$ is used as independent variable, the frequency f of the multipath pattern is constant assuming a locally planar and horizontal surface (Larson et al. 2008). The frequency $f = \frac{4\pi h}{\lambda}$ of the multipath modulation also depends on the reflector height h, which is the vertical distance between the ground reflecting planar surface and the electrical phase center of the antenna. It also depends on the wavelength λ of the GNSS carrier. The SNR of the multipath pattern can be described in terms of amplitude A and phase offset Φ by:

$$\mathrm{SNR} = A\cos\left(\frac{4\pi h}{\lambda}\sin\ e + \Phi\right) \tag{2}$$

In contrast to Larson et al. (2010), we do not restrict our analysis to satellites transmitting the L2C signal. In a first step, we included all satellites in the analysis. We partitioned the SNR in tracks per satellite number and azimuth quadrant. We also separated the SNR for satellites rising and setting on the same quadrant. For each satellite trace, we estimated the dominant frequency of the sinusoidal by applying the Lomb–Scargle periodogram method (Press and Rybicki 1989). This method allows calculating the spectral power for irregularly spaced time series. Figure 3, bottom panel, shows the Lomb–Scargle periodogram with the frequency converted into GNSS antenna height. We calculated a median reflector height separately for each track (combination of satellite PRN and azimuth). The median reflector height was then taken as a constant in the subsequent sinusoid fit. For some tracks the reflector height was systematically unstable. In these cases we excluded the combination of satellite PRN and azimuth for the entire time series, since presumably the ground does not conform well to the assumption of planar horizontal surface for these tracks. For estimation of soil moisture, the antenna height above the reflecting surface needs to be constant over time, both physically in the field (i.e., no moving platform) and later constrained to a constant value in data processing. The change in the antenna model did not affect the reflector height estimation. Hence, we fixed the reflector height to a constant value for the entire analysis period. Very few days with apparent antenna height, changes due to snow cover were excluded from the analysis. Snow was detected based on photos of the station surroundings. Tracks in east and south directions of the GNSS antenna were excluded from further processing due to the rocky boulders in this area. For a rough surface, the strength of the coherent part of the reflected signal decreases, while the diffuse scattering increases (Beckmann and Spizzichino 1987). For the interferometric technique, the coherent reflection component must be strong enough: only if the power of the dominant frequency is four times larger than the background noise and the satellite track contains more than 2000 data points (equal to roughly 30 min of observation) the track is included in the further processing.

In a next step we fitted a sinusoidal to the multipath interference and estimated amplitude and phase offset for the dominant frequency in a least-square adjustment. The derived phase offsets vary with time and are related to changes in the penetration depth of the reflected GNSS signal into the ground (Larson et al. 2008). This penetration depth strongly depends on the dielectric constant of the soil, which is related to the near-surface soil moisture (Nolan and Fatland, 2003; Larson et al. 2010).

Chew et al. (2013) modeled the GNSS signal penetration depth by using an electro-dynamic single-scattering forward model. The model was validated using field measurements of soil moisture at depths between 2.5 and 20 cm. The authors derived a linear relationship between SNR phase Φ and soil moisture with a slope of 65.1°/($\mathrm{cm}^3/\mathrm{cm}^3$). This means that a change of 1° in the phase corresponds to a change in volumetric water content of 0.015 $\mathrm{m}^3/\mathrm{m}^3$. The slope of this linear relationship varies by less than 0.003 $\mathrm{m}^3/\mathrm{m}^3$ for different soil types with diverse constituents of clay, sand and loam; thus, the relation is almost independent of the soil type. We used the above-mentioned regression function to convert the phase values of each single track into the corresponding soil moisture variations assuming the applicability of the regression function regardless of the antenna model. The equation used here to convert the phase changes $\Delta\phi$ into GNSS-derived Volumetric Water Content $\mathrm{VWC_{GPS}}$ ($\mathrm{m}^3/\mathrm{m}^3$) is:

$$\mathrm{VWC_{GPS}} = \frac{\Delta\phi}{65.1} + 0.05 \tag{3}$$

The phase changes $\Delta\phi = \phi - \phi_0$ are the difference in the phase ϕ with respect to a reference phase ϕ_0. Here, we used the minimum phase value as reference. The calibration of absolute soil moisture values is based on the assumption that the minimum soil moisture seen in the GNSS-derived time series corresponds to 0.05 $\mathrm{m}^3/\mathrm{m}^3$ (Larson, personal communication). Finally, we calculated a common mean of all satellite tracks that pass at different times during the day. The final soil moisture estimate represents a spatial and temporal average of all observations analyzed during one day (Figs. 4, 5). As the TDR observations were not used in the calibration process, they provide an independent option for validation.

The data of the station SUTM have a sampling rate of 1 s. However, the resolution of available data for many IGS stations in the archives, especially for the years of GPS

in the 1990s, is in general 30 s. The satellite needs about 1 h to pass from 5° to 30° elevation. Thus, for the time period of the satellite overpass, the number of observations is with 120 records very low for the 30-s data set compared to 3600 records in the 1-s data set. In order to estimate the impact of a lower sampling rate on the soil moisture estimates, we decreased the sampling resolution of the SUTM data to 5, 10 and 30 s. We analyzed all three datasets in the same way as described for the 1-s data set.

Validation

TDR measurements from December 2008 until September 2014 were used for validation. The validation study is based on data from L2P and L2C as these signals penetrate deeper into the soil than the L1 signal (Nolan and Fatland 2003). The more precise L2C signal was recorded only after May 7, 2013, when the GNSS receiver was upgraded. The soil moisture variations for the GNSS station SUTM were calculated as mean over the satellite tracks (PRN 2, 8, 14, 17, 23, 29). The standard deviation of the soil moisture from a single satellite track compared to the common mean is typically 0.06 m^3/m^3 VWC.

The temporal variations of the GNSS-derived soil moisture correspond very well to the TDR observations, both on daily and seasonal scales (Figs. 4, 5). For 2013, the soil moisture is low in the first 3 months of the year and higher after day 90 when a strong precipitation event occurred (Fig. 4). Small differences can be seen in the sensitivity of the two methods for small precipitation events. For example, the rainfall that occurred on day 123 (May 3) of 2013 causes a 0.04 m^3/m^3 increase in the VWC observed by GNSS. However, it does not affect the soil moisture recorded by the TDR sensors. The GNSS method is sensitive to the upper 0–5 cm, depending on the soil moisture content (Larson et al. 2008). In contrast, the vertical TDR probes record an integral value for a depth from 0 to 15 cm. This shows the high sensitivity of the GNSS method to small rain events, which are not detected by the TDR probes. It also indicates that the water from small precipitation events hardly infiltrates. The small precipitation event is also not visible in the observations of the horizontally installed TDR sensors at 10 cm depths. Even larger rainfall events can be expected to infiltrate into the top layer only, as illustrated by the dye tracer experiments (Fig. 6). For the artificial rainfall volume of 17 mm (exceeded by only 5 % of all natural daily rainfall volumes in the study period), average infiltration depth was about 5 cm, with very few individual flow paths to depths of 15–20 cm. After the precipitation events, soil moisture from GNSS signals decreases faster than the soil moisture from TDR. This is also related to the deeper integration depth of the TDR measurements. The GNSS observations, in contrast, are sensitive to the uppermost soil layer only which dries out more quickly due to evaporation.

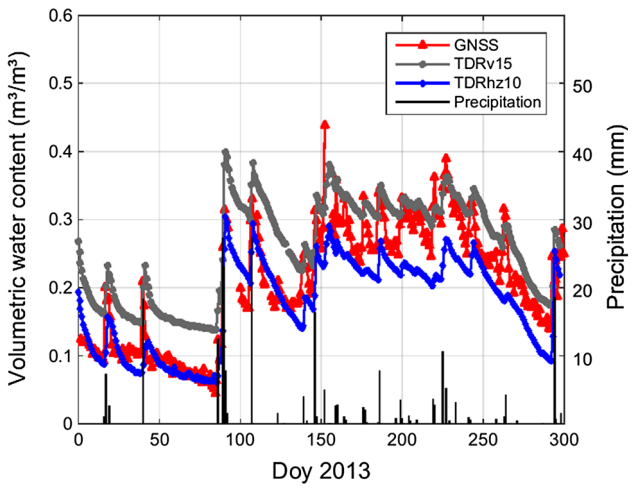

Fig. 4 Comparison of daily soil moisture from GNSS data (average of L2P and L2C) and TDR sensors, with daily precipitation amounts on the right *y*-axis. TDRv15 represents the average of nine vertically installed sensors giving integrated values over the top 15 cm of the soil. TDRhz10 shows the average of four horizontally placed sensors at a soil depth of 10 cm

The 6-year period of this study illustrates the strong seasonal soil moisture dynamics in Sutherland, based on both GNSS and TDR data (Fig. 5). The near-surface soil tends to wet up by about 0.2 m^3/m^3 during the winter season and stays in a wet state for several weeks or months. Exceptions are the comparatively dry years 2010 and 2014 where this wet state is not reached and rainfall events tend to cause single short soil moisture peaks with subsequent drying to a low soil moisture status. Throughout the entire study period, intense rainfall events in particular during the summer season may result in pronounced but short-term soil moisture peaks (Fig. 5).

The GNSS-derived Volumetric Water Content (VWC_{GNSS}) and the soil moisture from the TDR sensors (VWC_{TDR}) are highly correlated with a correlation coefficient of 0.8 (Table 1). The regression analysis shows that VWC_{GNSS} is on average drier than VWC_{TDR} by 0.10 m^3/m^3 for the vertically placed TDR sensors extending over the top 15 cm (TDRv15) and by 0.03 m^3/m^3 for the horizontally installed TDR sensors at 10 cm depths (TDRh10) (Fig. 7). From the soil moisture difference between 10 and 20 cm depth, it can be seen that soil moisture tends to be higher at greater depth during most of the time (Fig. 8). However, the relationship is reversed during individual short periods in the course of rainfall events where quick infiltration reaches the 10 cm sensor only, or where longer infiltration times to the deeper sensor lead to a delayed response at 20 cm.

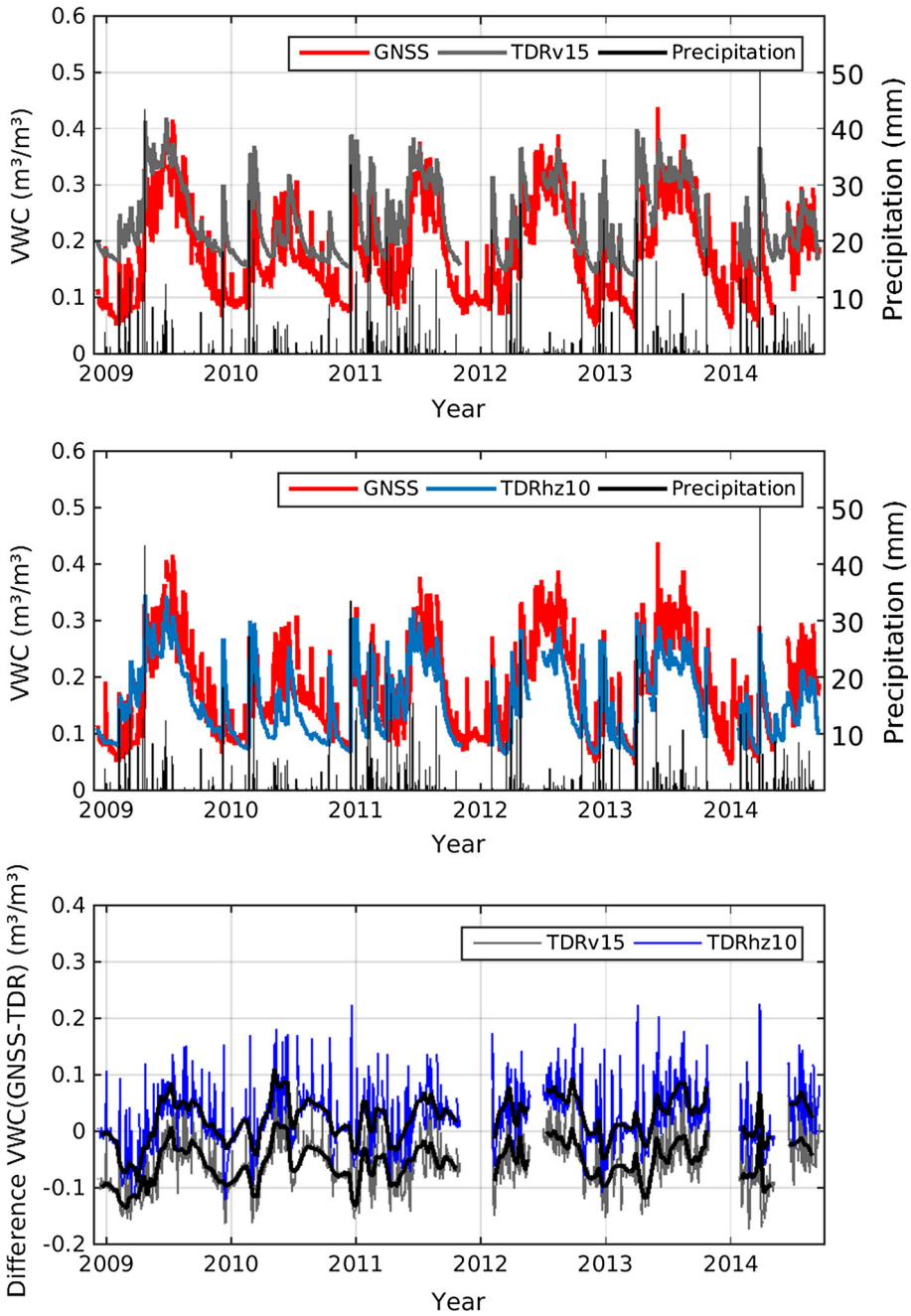

Fig. 5 Comparison of soil moisture from GNSS data (average of L2P and L2C) and TDR sensors. *Top panel* shows average values of nine TDR sensors integrating over a depth from 0 to 15 cm. *Middle panel* shows average values of four TDR sensors at the depth of 10 cm, and daily precipitation. The GNSS soil moisture estimates are continuous in time and also provide information on soil moisture dynamics when the TDR system has data gaps, e.g., end of 2011 and 2013. *Bottom panel* shows the difference in soil moisture between TDR and GNSS: daily values and monthly moving mean

For the GNSS observations, the penetration depth depends on the soil moisture content. The drier the soil, the deeper the signal penetrates into the soil. For dry periods, e.g., during the days 60–90 in 2013, the VWC_{GNSS} corresponds very well to VWC_{TDR} from the sensors at 10 cm depths (Fig. 4). This confirms that the tuning of the time series to a minimum soil moisture value of 0.05 m^3/m^3 (see section "Data Analysis") seems to be a reasonable approximation for the Sutherland site. For the validation of VWC_{GNSS}, the TDR sensors at 10 cm depth can be considered as the most suitable ones as they are closest to the surface of all available sensors and less influenced by deeper soil moisture in comparison with the TDRv15 sensors. The accuracy of the VWC_{GNSS} derived from the comparison with the TDRh10 sensors is 0.05–0.06 m^3/m^3 (RMSE in Table 1).

The residuals VWC_{GNSS}–VWC_{TDR} show a dependency on the soil moisture content (Fig. 5 bottom panel, Fig. 9). The residuals (VWC_{GNSS}–VWC_{TDRv15}) as well as the residuals (VWC_{GNSS}–$VWC_{TDRhz10}$) correlate with the GNSS soil moisture content by $r^2 = 0.57 \pm 0.03$ and by $r^2 = 0.70 \pm 0.06$, respectively. VWC_{GNSS} and $VWC_{TDRhz10}$ agree better for dryer than for wetter conditions (Fig. 5 bottom panel). One reason for the dependency

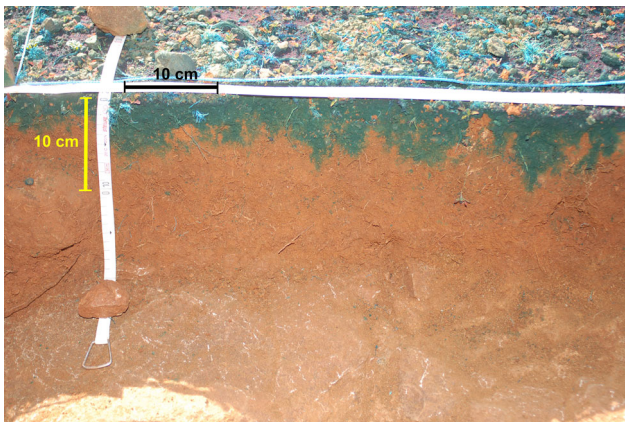

Fig. 6 Infiltration pattern at a site located about 30 m north of the GNSS station. Flow paths are visualized with the dye trace "Brilliant Blue". Soil depth at this site is approximately 20 cm, excavated bedrock can be seen in the lower part of the photograph

of the residuals with soil moisture could be the uncertainty of the calibration factor, which relates the phase observations to the soil moisture content. The different regression coefficients of 2.15 and 1.81 for the AOAD/M T and Javad antenna indicate that the calibration coefficient may vary with the antenna type. Here, however, we used one calibration factor for the entire time period. Another reason for larger residuals in weather conditions could be that the penetration depth of the GNSS signal depends on the soil moisture content. With a larger penetration depth during dryer conditions, the measured soil moisture with the TDRhz10 sensors at a depth of 10 cm can be expected to be more representative for the GPS-based soil moisture than for weather conditions where the GNSS signal penetrates into the uppermost centimeters only, causing larger residuals.

Effect of antenna change

The replacement of the antenna at station SUTM on May 7, 2013, caused an offset in the GNSS soil moisture time series at the day of the antenna change by 0.19 and 0.08 m^3/m^3 for the soil moisture estimated from L1 and L2P, respectively. One possible reason for the observed offset could be related to different phase centers of the new and old antenna. A change in the phase center could cause a change in the observation geometry, similar to the antenna being at a different height. Small changes in reflector height, if unaccounted for, will be absorbed by the phase-shift parameter since frequency and phase are correlated parameters. As the time series of the estimated reflector heights for all satellites used show no change before and after the day of the antenna change, we fixed the reflector height in the subsequent phase-shift estimation for the whole processing period. Another possible reason for the observed offset in the GNSS soil moisture time series could be a change in the antenna gain pattern.

After the antenna change, the absolute soil moisture values were tuned again to the assumption of a minimum soil moisture of 0.05 m^3/m^3. For short time periods of less than 1 year, the data may not cover the dry season and the assumption made above might not be valid anymore. Another possibility is the correction of the offsets by assuming that the soil moisture during the day of the antenna change did not change significantly, which is only justified if there is no rainfall on this day. For Sutherland, no precipitation was recorded during the day of antenna change. The difference between the recalibrated time series and the time series corrected by the offset estimated from subsequent days is less than 0.01 m^3/m^3 for L1 and L2. The good agreement between both methods is related to optimal conditions: no rain plus data coverage of dry seasons both before and after the antenna change. In the case that less data are available which do not cover the dry season or if the year is exceptionally wet, the calibration might be biased. For a rainy day during antenna change the offset correction might also cause a bias in the soil moisture.

In addition to the additive bias we checked for a multiplicative bias. The comparison of the VWC_{GNSS} with VWC_{TDRv15} shows a larger regression slope of 0.78 ± 0.01 for the AOAD/M T antenna compared to a slope of 0.72 ± 0.01 for the JAVAD antenna. Also the regression analysis with $VWC_{TDRhz10}$ reveals with 0.78 ± 0.02 a larger slope for the AOAD/M T antenna

Table 1 Comparison of the soil moisture estimates from GNSS and TDR

	Correlation r^2	Regression slope	Regression intercept (m^3/m^3)	RMSE (GNSS-TDR) (m^3/m^3)
TDRv15 AOAD/M T	0.82 ± 0.02	0.78 ± 0.01	0.10 ± 0.002	0.07
TDRhz10 AOAD/M T	0.78 ± 0.02	0.78 ± 0.01	0.02 ± 0.003	0.05
TDRv15 JAVAD	0.75 ± 0.05	0.72 ± 0.03	0.10 ± 0.006	0.07
TDRhz10 JAVAD	0.76 ± 0.05	0.65 ± 0.03	0.04 ± 0.006	0.06

The statistics refer to the scatter plot in Fig. 7

The confidence interval is based on a 95 % level of significance

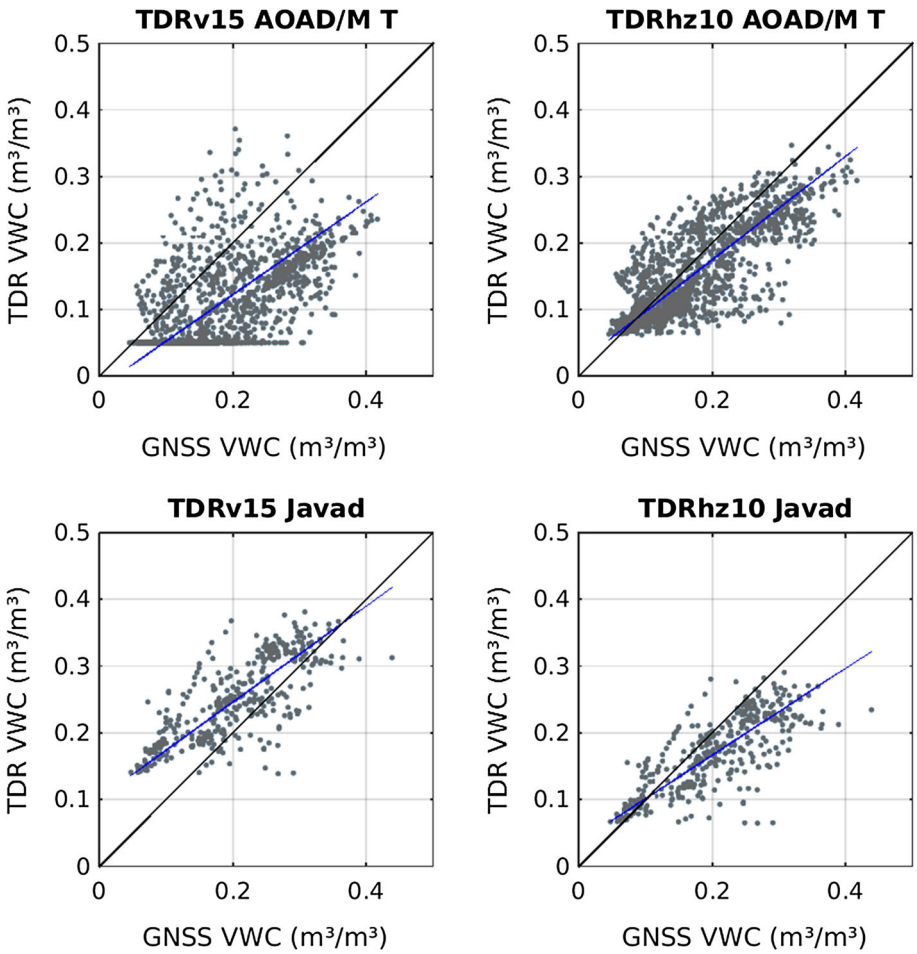

Fig. 7 Scatter plot of the soil moisture from GNSS data and TDR sensors. *Upper panels* show the comparison for GNSS data from the AOAD/M T antenna for the period from December 5, 2008, to May 7, 2013. *Lower panels* show the comparison for GNSS data from the Javad antenna for the period from May 7, 2013, to September 12, 2014. *Left panels* refer to the vertically installed TDR sensors giving integrated values over a depth from 0 to 15 cm (TDRv15), and *right panels* refer to the horizontally placed sensors at 10 cm depths (TDRhz10). *Blue line* represents the regression line and *black line* the ideal 1:1 line. Statistics on the comparison are given in Table 1

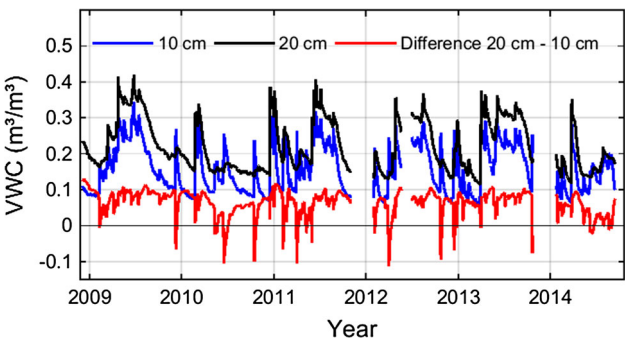

Fig. 8 Mean soil moisture at 10 and 20 cm depths (each is an average of four horizontally placed TDR sensors) and difference between both time series (*red line*)

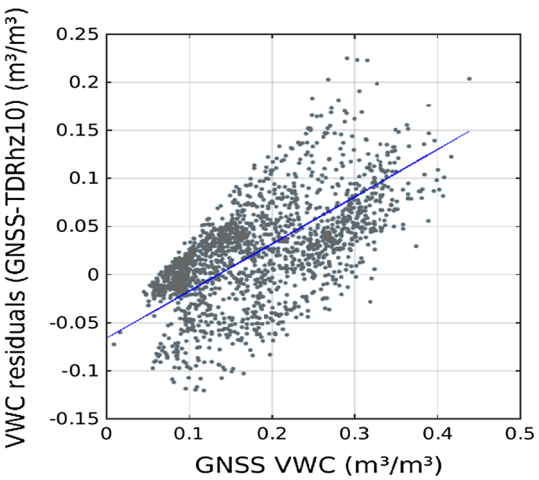

Fig. 9 Scatter plot of the soil moisture residuals (VWC from GNSS-VWC from TDR sensors at 10 cm depth, see Fig. 5 *bottom panel*) compared to the soil moisture from GNSS. The *blue line* represents the regression line

compared to 0.65 ± 0.02 for the JAVAD antenna (Table 1). The differences in the regression slopes of up to 0.13 indicate a slight dependency of the calibration coefficient on the antenna model. The time period for the GNSS observation with the AOAD/M T covers more than 4 years, while data for the Javad antenna are analyzed for less than 1 year. Since the longer AOAD/M T data set covers the full range of soil moisture variations, it is the most suitable for an error estimation of the GNSS soil moisture.

Comparison of GNSS soil moisture results for L1, L2P and L2C

For the particular antenna used in this study, the L1 signal has a similar signal strength as the L2C signal transmitted by the newer satellites (Fig. 10). However, the SNR from L1 is less precise than the SNR for L2C, with more noise in the interference pattern in particular at higher elevation angles between 20 and 30 ° (Fig. 10). The L2P signal is 20 dB weaker, which means 100 times weaker as L2C. Since the L2C signal provides the highest signal strength and precision, previous studies focused mainly on L2C signals or the upcoming L5 signal (Larson et al. 2010; Tabibi et al. 2015).

However, the SNR of the L1 and L2P signal also shows interference patterns (Fig. 10). The SNR of L2P is a more distorted, showing less sinusoidal interference pattern because the SNR of L2P exhibits significant auto-correlation. Nevertheless, the parameters of the frequency, amplitude and phase can clearly be identified from the SNR of the L1 and L2P signal using (2). The standard deviation from the least-square adjustment of the phase estimates is 0.71°, 0.78° and 0.44° for the L1, L2P and L2C signal. Since the elevation angles at which the observations are collected are the same for all signals, their design matrices are also the same; thus, the difference in the parameter uncertainty can only arise from the scaling of the covariance matrix diagonal by the RMSE of the residuals. This interpretation corroborates with the smaller uncertainty in the phase estimates for the L2C SNR, which is the least noisy one. The standard deviation of the phase estimates translates by factor 1.5 into the precision of the VWC estimates corresponding to 0.011, 0.012 and 0.007 m^3/m^3, respectively. Even if the precision of the soil moisture estimates from L2C is better by nearly a factor of two than for L1 and L2P, the precision of the soil moisture derived from L1 and L2P is still good enough for most hydrological applications.

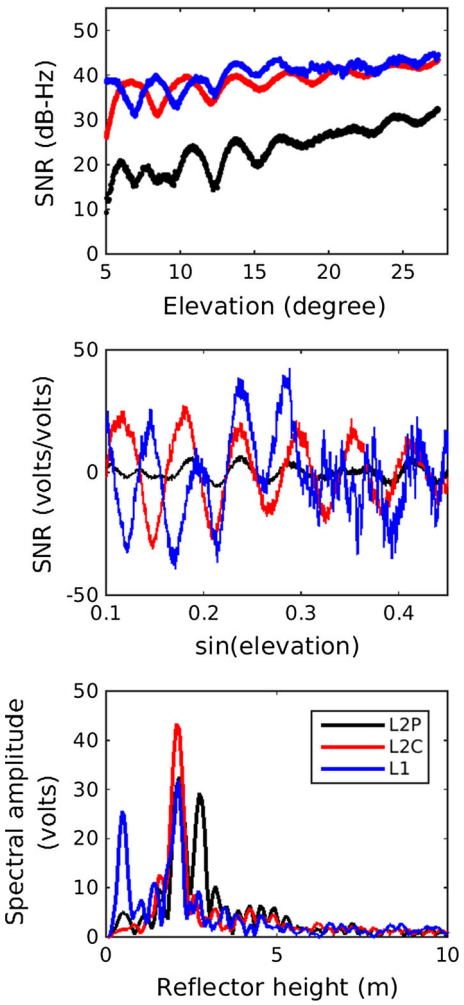

Fig. 10 Comparison of the signal-to-noise ratio (SNR) of the L1, L2P and L2C signals for the GPS satellite PRN 17. *Top panel* shows the SNR of the complete signal (direct and reflected), *middle panel* refers to the SNR of the reflected signal converted to volts/volts, *bottom panel* presents the Lomb–Scargle periodogram of the SNR from the reflected signal

Soil moisture time series derived from the L1, L2P and L2C signals all reproduce the wetting and drying cycles in response to rainfall (Fig. 11). Since the SNR from the L2C signal gives the most precise solution, we used this as reference and compared the soil moisture estimates from the L1 and L2P signal against L2C. The RMSE of the differences in soil moisture is 0.03 m^3/m^3 between both, L2C and L1 as well as L2C and L2P. There are small inter-frequency and inter-code biases in the GPS soil moisture retrievals of -0.02 m^3/m^3 for L1 and L2C and 0.01 m^3/m^3 for L2P and L2C. Larger differences between L2C and L1 compared to L2P can be related to the different penetration depth of the L1 signal. The L1 signal with a wavelength of 19.05 cm has a smaller penetration depth than the L2P and L2C signal with a wavelength of 24.45 cm. This is consistent with the slightly higher correlation between L2C and L2P with 0.96 ± 0.01 compared to the correlation of 0.91 ± 0.02 for L2C and L1. The regression slope for L2C/L2P is with 1.12 ± 0.01 different from the regression slope of L2C/L1 with 1.03 ± 0.01. Hence, the calibration seems to be carrier frequency dependent.

Both the L1 and L2P signals are suitable for soil moisture estimation, especially for older GNSS records, where no L2C observations are available. In the case of SUTM, the L2C has been only available since May 2013, when the new receiver was installed (see "GNSS data" section). Additionally, the spatial coverage was improved. By including observations from older satellites that are transmitting the L2P signal only, the number of scans per day increased by a factor of three from two to six scans.

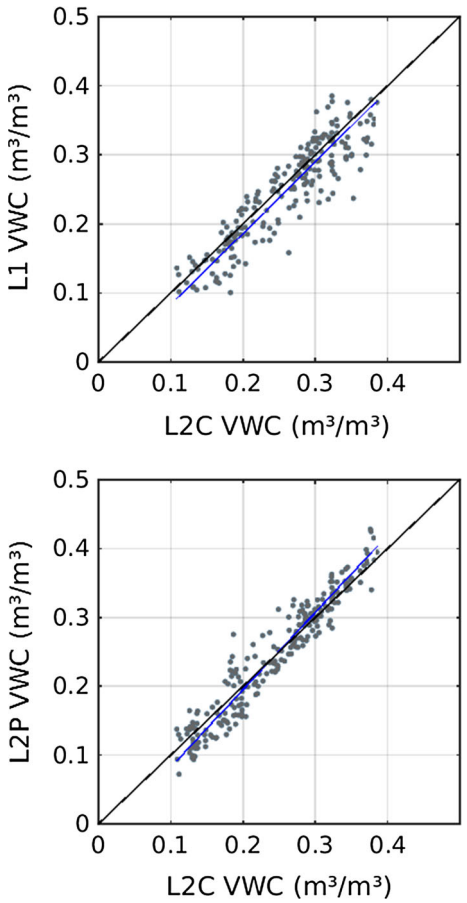

Fig. 11 Comparisons of the soil moisture, estimated from the L1 and L2P data with those from L2C signals of the GPS satellite PRN 17 for the period May 7–December 31, 2013. The *blue line* represents the linear regression result and the *black line* the ideal 1:1 line

Effect of the data sampling rate

The analysis step of fitting a sinusoidal to the SNR data depends on the sampling rate. The precision of the phase, estimated by least-square adjustment using (2), strongly decreases from 0.5°, 1°, 1.8° to 2.5° with lowering of the sampling interval from 1, 5, 10 to 30 s, respectively. The three down-sampled solutions were compared with the 1-s solution as reference (Fig. 12). The soil moisture retrievals from the 30-s data can differ in some cases up to 0.04 m^3/m^3 from the 1-s soil moisture estimates. The RMSE of the differences in soil moisture is 0.006, 0.0012 and 0.013 m^3/m^3 for the estimates of the 5-, 10- and 30-s data sets compared to the 1-s data set, respectively. The regression analysis of the 1-s solution with the down-sampled solutions reveals a correlation of better than 0.99 ± 0.003, a regression slope of 0.98–1 and a bias smaller than 0.001 m^3/m^3 for all sampling rates. For soil moisture estimation, the high-rate 1-s GNSS observations are preferable as they give

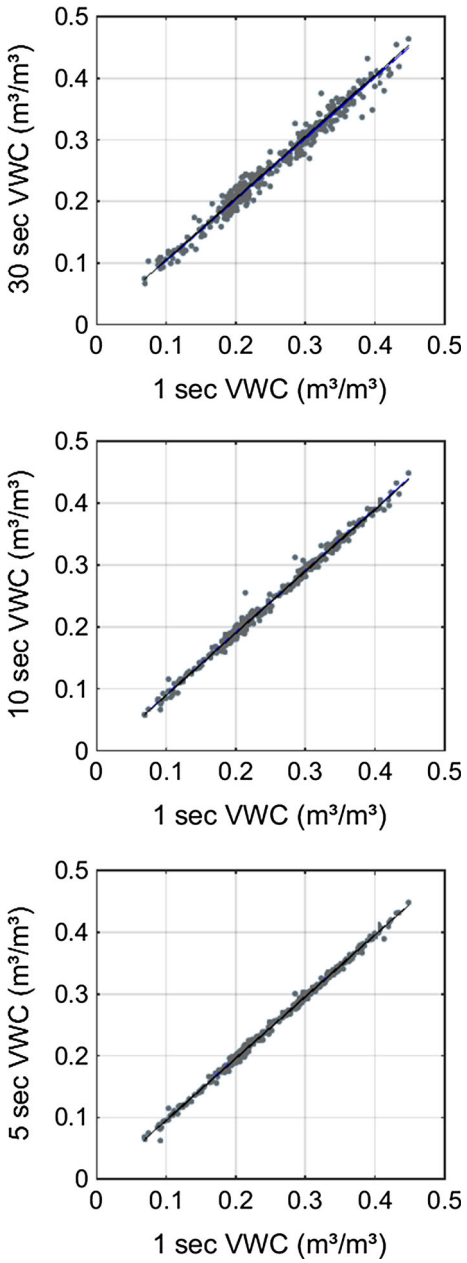

Fig. 12 Comparison of soil moisture derived from GNSS data with 5-, 10- and 30-s sampling rates for the period January 1–December 31, 2013. The *blue line* represents the linear regression line

the most precise results. However, when the high-resolution data are not available, the differences for the soil moisture derived from the 30-s data are small with an RMSE of 0.01 m^3/m^3. The effect of sampling rate is expected to be dependent on the reflector height. With a larger reflector height, the frequency of the interference pattern increases. The results presented here for an antenna 2 m above terrain surface are not necessarily valid for antenna setups much higher than that, e.g., for roof-top installations.

Conclusions

This case study with the longest GNSS-based soil moisture time series published to date shows that temporal variations of near-surface soil moisture estimated from GNSS data at the IGS station SUTM capture the soil moisture increase due to precipitation events and the subsequent drying due to evapotranspiration very well. The data from the horizontal TDR sensors at 10 cm depth and the GNSS soil moisture time series from the AOAD/M T antenna, covering more than 4 years, seem to be the most suitable for the GNSS soil moisture validation, resulting in an overall accuracy of GNSS-derived soil moisture of 0.05 m^3/m^3 (RMSE in Table 1). The GNSS-derived soil moisture estimates are highly correlated with the soil moisture variations observed by TDR sensors. Deviations between the GNSS and TDR datasets are primarily due to the fact that TDR sensors are installed at deeper soil depths and soil moisture is generally increasing with depth and also becomes less sensitive to precipitation events with depth. Despite these deviations, the good agreement implies that the GNSS soil moisture estimates can fill data gaps in the TDR time series. Additionally, for sites without TDR sensors, permanent GNSS stations with similar environmental conditions could provide near-surface soil moisture data. Thus, the already existing worldwide network of geodetic GNSS receivers has a great potential to complement the existing dedicated soil moisture-monitoring networks.

The SNR of the L1 and L2P signals from geodetic antennas can provide reliable soil moisture estimates, which are less precise than the L2C signal. The comparisons of the soil moisture estimates from the SNR of the L1 and L2C signals as well as from L2P and L2C signals show differences with an RMSE of 0.03 m^3/m^3. Extending the soil moisture estimation to the L1 and L2P signals has the strong advantage that it broadens the applicability of the soil moisture estimation to historical GNSS observations when no L2C signal was available. Another advantage of using L1 signals is that L1-only GNSS receivers are much cheaper than geodetic dual-frequency receivers and could be used to increase the density of network observations.

Historic GNSS data are mainly stored with 30-s temporal resolution. The soil moisture derived from the 30-s data differs very little from the soil moisture derived from the 1-s data with an RMSE of their deviations of 0.01 m^3/m^3. This implies that the 30-s data provide a unique data source to study seasonal and inter-annual soil moisture changes since many of these stations provide continuous data over the past two decades. At long-term monitoring stations, GNSS equipment usually needs to be replaced or updated at some point. The change in GNSS antennas may cause an additive bias of more than 0.1 m^3/m^3. There is also a small dependence of the GNSS-TDR regression slope on the antenna model. Possible causes for the antenna type dependence of the soil moisture retrievals, e.g., the impact of different antenna phase center or the antenna gain pattern, need to be investigated further.

In future, soil moisture estimates based on GNSS signals could be obtained in near real time and assimilated into hydrological models or numerical weather prediction models as an important descriptor of the state of the land surface. They could also provide a valuable database to validate soil moisture estimates from other sensors like COSMIC ray sensor networks or from satellite missions (Dorigo et al. 2014).

Data supplement

The GNSS-based soil moisture time series for the station Sutherland, South Africa, is made available for the time period of this study (January 1, 2008, to September 1, 2014). It provides the integral soil moisture over an area of 60 by 60 m for the uppermost surface (max. down to 10 cm depth). The data are daily averages based on daily measurements from six different satellites (Vey et al. 2015).

Acknowledgments We thank Kristine Larson for her helpful advice and discussions, Benjamin Creutzfeldt, Pieter Fourie and Jaci Cloete for their help in the field with sensor installation and maintenance, the South African Astronomic Observatory for their hospitality and support and acknowledge the Helmholtz Alliance HA310 "Remote Sensing of Earth System Dynamics" (HGF EDA) for funding the first author of this study. Reviewers are gratefully acknowledged for their comments.

References

Alonso-Arroyo A, Camps A, Aguasca A, Forte GF, Monerris A, Rudiger C, Walker JP, Park H, Pascual D, Onrubia R (2014) Dual-polarization GNSS-R interference pattern technique for soil moisture mapping. IEEE J Sel Top Appl Earth Obs Remote Sens 7(5):1533–1544. doi:10.1109/JSTARS.2014.2320792

Beckmann P, Spizzichino A (1987) The scattering of electromagnetic waves from rough surfaces. Artech House Radar Library

Brocca L, Melone F, Moramarco T, Wagner W, Naeimi V, Bartalis Z, Hasenauer S (2010) Improving runoff prediction through the assimilation of the ascat soil moisture product. Hydrol Earth Syst Sci 14(10):1881–1893. doi:10.5194/hess-14-1881-2010

Chew CC, Small EE, Larson KM, Zavorotny VU (2013) Effects of near-surface soil moisture on gps snr data: development of a retrieval algorithm for soil moisture. IEEE Trans Geosci Remote Sens 52(1):537–543. doi:10.1109/TGRS.2013.2242332

Dorigo WA et al (2014) Evaluation of the ESA CCI soil moisture product using ground-based observations. Remote Sens Environ. doi:10.1016/j.rse.2014.07.023

Drusch M (2007) Initializing numerical weather prediction models with satellite-derived surface soil moisture: data assimilation experiments with ECMWF's integrated forecast system and the TMI soil moisture data set. J Geophys Res 112(D3):3102. doi:10.1029/2006JD007478

Egido A, Paloscia S, Motte E, Guerriero L, Pierdicca N, Caparrini M, Santi E, Fontanelli G, Floury N (2014) Airborne GNSS-R polarimetric measurements for soil moisture and above-ground biomass estimation. IEEE J Sel Topics Appl Earth Obs Remote Sens 7(5):1522–1532. doi:10.1109/JSTARS.2014.2322854

Entekhabi D, Njoku E, O'Neill P, Spencer M, Jackson T, Entin J, Im E, Kellogg K (2008) The soil moisture active/passive mission (SMAP). Geosci Remote Sens Symp IGARSS IEEE Int 98(5):704–716. doi:10.1109/JPROC.2010.2043918

Fontana RD, Cheung W, Novak PM, Thomas A (2001) The new L2P civil signal. In: Proceedings of ION ITM GPS Institute of Navigation, September, Salt Lake City UT, pp 617–631

Gurtner W, Estey L (2007) RINEX: The receiver independent exchange format version 2.11. http://igscb.jpl.nasa.gov/igscb/data/format/rinex211.txt

Katzberg SJ, Torres O, Grant MS, Masters D (2005) Utilizing calibrated GPS reflected signals to estimate soil reflectivity and dielectric constant: results from SMEX02. Remote Sens Environ 100(1):17–28. doi:10.1016/j.rse.2005.09.015

Larson KM, Nievinski FG (2012) GPS snow sensing: results from the earthscope plate boundary observatory. GPS Solut 17(1):41–52. doi:10.1007/s10291-012-0259-7

Larson KM, Small EE, Gutmann E, Bilich A, Axelrad P, Braun J (2008) Using GPS multipath to measure soil moisture fluctuations: initial results. GPS Solut 12(3):173–177. doi:10.1007/s10291-007-0076-6

Larson KM, Braun JJ, Small EE, Zavorotny VU, Gutmann ED, Bilich AL (2010) GPS multipath and its relation to near-surface soil moisture content. IEEE J Sel Topics Appl Earth Obs Remote Sens 3(1):91–99. doi:10.1109/JSTARS.2009.2033612

Martin-Neira M (1993) A passive reflectometry and interferometry system (PARIS): application to ocean altimetry. ESA J 17(4):331–355

Masters D, Axelrad P, Katzberg S (2002) Initial results of land-reflected GPS bistatic radar measurements in SMEX02. Remote Sens Environ 92(4):507–520. doi:10.1016/J.RSE.2004.05.016

Nievinski FG, Larson KM (2014) Forward modeling of multipath for near-surface reflectometry and positioning applications. GPS Solut 18(2):309–322. doi:10.1007/s10291-013-0331-y

Nolan M, Fatland DR (2003) Penetration depth as a DInSAR observable and proxy for soil moisture. IEEE Trans Geosci Remote Sens 41(3):532–537. doi:10.1109/TGRS.2003.809931

Perry MA, Niemann JD (2008) Generation of soil moisture patterns at the catchment scale by EOF interpolation. Hydrol Earth Syst Sci 12(1):39–53. doi:10.5194/hess-12-39-2008

Press WH, Rybicki GB (1989) Fast algorithm for spectral analysis of unevenly spaced data. Astrophys J 338:277–280. doi:10.1086/167197

Rodriguez-Alvarez N, Camps A, Valencia E, Hernandez JM, Perez I (2009) Soil moisture retrieval using GNSS-R techniques: experimental results over a bare soil field. IEEE Trans Geosci Remote Sens 47(11):3616–3624. doi:10.1109/TGRS.2009.2030672

Schaufler G, Kitzler B, Schindlbacher A, Skiba U, Sutton MA, Zechmeister-Boltenstern S (2010) Greenhouse gas emissions from European soils under different land use: effects of soil moisture and temperature. Eur J Soil Sci 61(5):683–696. doi:10.1111/j.1365-2389.2010.01277.x

Seneviratne SI, Corti T, Davin EL, Hirschi M, Jaeger EB, Lehner I, Orlowsky B, Teuling AJ (2010) Investigating soil moisture–climate interactions in a changing climate: a review. Earth-Sci Rev 99(3–4):125–161. doi:10.1016/j.earscirev.2010.02.004

Tabibi S, Nievinski FG, van Dam T, Monico JFG (2015) Assessment of modernized GPS L5 SNR for ground-based multipath reflectometry applications. Adv Space Res 55(4):1104–1116. doi:10.1016/j.asr.2014.11.019

Topp GC, Davis JL, Annan AP (1980) Electromagnetic determination of soil water content: measurements in coaxial transmission lines. Water Resour Res 16(3):574–582. doi:10.1029/WR016i003p00574

Vey S, Güntner A, Wickert J, Blume T, Ramatschi M (2015) Supplement to: long-term soil moisture dynamics derived from GNSS interferometric reflectometry: a case study for Sutherland, South Africa. GFZ German Research Center for Geosciences. doi:10.5880/GFZ.1.1.2015.001

Wanders N, Karssenberg D, de Roo A, de Jong SM, Bierkens MFP (2014) The suitability of remotely sensed soil moisture for improving operational flood forecasting. Hydrol Earth Syst Sci 18:2343–2357. doi:10.5194/hess-18-2343-2014

Wang L, Qu JJ (2009) Satellite remote sensing applications for surface soil moisture monitoring: a review. Front Earth Sci China 3(2):237–247. doi:10.1007/s11707-009-0023-7

Zavorotny VU, Masters D, Gasiewski A, Bartram B, Katzberg S, Axelrad P and Zamora R (2003) Seasonal polarimetric measurements of soil moisture using tower-based GPS bistatic radar. In: Proceedings of IEEE 2003 international geoscience and remote sensing symposium, IGARSS 2003, vol 2, pp 781–783. doi:10.1109/IGARSS.2003.1293916

Sibylle Vey is a postdoctoral researcher at GFZ Potsdam, Germany, where she works in the field of GNSS multipath reflectometry. She earned her Ph.D. (Geodesy) from the University of Technology Dresden, Germany, in 2008.

Andreas Güntner is a senior scientist in the Section of Hydrology at GFZ Potsdam, Germany, and professor for hydro-gravimetry at Potsdam University. He earned his Ph.D. (Hydrology) from Potsdam University in 2002.

Jens Wickert is a GFZ senior scientist and expert in the application of GNSS signals for remote sensing of the earth's atmosphere and surface (www.Jenswickert.de). He received his Ph.D. degree in Geophysics and Meteorology from the Karl-Franzens University Graz, Austria, in 2002.

Theresa Blume is a senior scientist in the Section of Hydrology at GFZ Potsdam, Germany. Her research interests include the investigation of hydrological and eco-hydrological processes using innovative experimental methods, experimental designs and monitoring networks. She earned a Ph.D. in hydrology from Potsdam University in 2007.

Markus Ramatschi is a senior scientist at GFZ Potsdam, Germany. His work focuses mainly on the operation of GNSS sensor stations. He earned his Ph.D. (Geophysics) from the Technical University of Clausthal, Germany, in 1998.